Analytical Biochemistry 583 (2019) 113365

Contents lists available at ScienceDirect

Analytical Biochemistry

journal homepage: www.elsevier.com/locate/yabio

DNA-silver nanocluster probe for norovirus RNA detection based on changes in secondary structure of nucleic acids

Fumiao Shen[a], Yuliang Cheng[a], Yunfei Xie[a], Hang Yu[a], Weirong Yao[a], Hung-Wing Li[b], Yahui Guo[a,*], He Qian[a]

[a] State Key Laboratory of Food Science and Technology, School of Food Science and Technology, Jiangnan University, Wuxi, 214122, China
[b] Department of Chemistry, Hong Kong Baptist University, Kowloon Tong, Hong Kong, China

ARTICLE INFO

Keywords:
Biosensor
DNA-templated silver nanoclusters
Fluorescence
RNA detection
Label-free

ABSTRACT

DNA-templated silver nanoclusters (DNA-AgNCs) is a kind of fluorescent nanoclusters in-situ synthesized on DNA, thereby giving the DNA probe an inherent function of label-free signal output. Herein, the DNA-AgNCs with a GCC-loop-structure which has a quantum field of 51.6% was firstly proposed. It was proved that the addition of the double-stranded structure on the GCC-loop drastically enhanced the fluorescence intensity of the AgNCs. Through the further studies of the relationship between DNA secondary structure and AgNCs, a kind of DNA-AgNCs-probe was designed based on the change of the secondary structure which was induced by the target strand. By this, the fluorescence signal of probe was in "turn on" mode. The probe system could be directly used for the detection of Norovirus RNA, which had a linearity of 20 nM to 1.8 μM with a detection limit of 18 nM. Moreover, this detection platform was also selective to differentiate mismatched RNA. It was expected to be a universal method for different RNA detection by changing the recognition sequence of the probe.

1. Introduction

Norovirus is a member of the family Caliciviridae and is the major cause of acute viral gastroenteritis worldwide, commonly known as "winter vomiting disease" and has been identified as the predominant cause of food-borne outbreaks [1–3]. Both food and water are important sources of norovirus transmission. Rapid and accurate detection is important for diagnosis of norovirus in patients and for tracing the source of the virus in food and environmental samples. The early diagnosis methods of Norovirus mainly include direct electron microscopy and immunoelectron microscopy (IEM). Because of the low sensitivity and specificity of these methods [4], many cases of Norovirus infection cannot be diagnosed. Nucleic acid is one of the most basic substances in life. Research and development based on nucleic acid detection methods had made polymerase chain reaction (PCR) especially Real-time PCR (RT-PCR) [5–8] the most routine and highly specific Norovirus RNA detection methods. Although a number of alternative methods for Norovirus detection have been reported, electrochemical [3], ELISA [9], dot-blotting [10], NanoZyme aptasensor [11] etc. These methods have good sensitivity, but there are also many problems, such as complicated operation, the use of enzymes, high costs, electrode modification, enzyme modification, and difficulty in synthesis etc. This research aimed to establish a universal, simple, label-free method for rapid detection of Norovirus RNA.

The developments in nanotechnology have seen the emergence of colorimetric and other potential biosensing platforms as a viable technology for point-of-care devices [12,13]. Silver nanoclusters (AgNCs), in particular, have been at the forefront due to well-established synthesis routes, low toxicity, smaller than semiconductor quantum dots and better photostability and brightness than commonly used organic dyes [14–16]. DNA is an excellent type of template which can conveniently encode the emission spectrum of AgNCs by sequence and conformational changes of the DNA scaffold [17,18]. SsDNA [19], dsDNA [20], DNA hairpin [21], triplex DNA [22], I-Motif Folding [23], G-quadruplex [24] et al. had been used to synthesize AgNCs. In the other way, functionalization of the luminophore could be easily accomplished to facilitate biorecognition through hybridization or aptamer-target recognition of extended sequences [25–27]. However, DNA templated AgNCs (DNA-AgNCs) with high quantum yield and excellent optical properties are rare, which limited its applications. In this work, based on the study of detection strategies for DNA probes of different sequences, a DNA template which can be used to synthesize AgNCs with a quantum yield of 51.60% was firstly used.

With the development of detection technology, it is increasingly

* Corresponding author.
E-mail address: guoyahui@jiangnan.edu.cn (Y. Guo).

https://doi.org/10.1016/j.ab.2019.113365
Received 22 May 2019; Received in revised form 15 July 2019; Accepted 16 July 2019
Available online 17 July 2019
0003-2697/

necessary to develop a more convenient, novel and sensitive detection method of RNA. In the current study, we designed a label-free DNA-AgNCs-probe with identification and signal output capabilities which can be easily used to specifically detect Norovirus RNA. This method did not require enzymes or chemical modification, it was only necessary to mix the target RNA with the probe solution to incubate for a period of time, and then generated a strong fluorescent signal changing by simple AgNCs synthesis. It was found through the research that the change of fluorescence signal was due to the change of DNA secondary structure of DNA-AgNCs. The DNA probe formed a GCC-loop which could be used to synthesize AgNCs with high quantum yield. And the fluorescence intensity of the GCC-loop AgNCs was significantly enhanced by the additional of double-strand structure.

2. Experimental

2.1. Reagents

The oligonucleotides used in this work were all synthesized by Sangon Biotech Co. (Shanghai, China) and the sequences were listed in Table S1. The stock solution of DNA/RNA samples was prepared in ultrapure water, and the DNA/RNA concentration was accurately quantified based on 260 nm UV absorbance. $AgNO_3$, $NaBH_4$, NaH_2PO_4 and Na_2HPO_4 were of analytical grade and used without further purification. Millipore Milli-Q (18 MΩ cm) water was used in all experiments.

2.2. Reaction for RNA assay and synthesis of AgNCs

The DNA-AgNCs were created as follows: the probe (2 μM) and target RNA of different concentrations were mixed in sodium phosphate buffer (20 mM, pH 6.6) for 30min; then $AgNO_3$ (final concentration 24 μM) were added to the mixture solution and incubated at 4 °C for 30 min (under dark); Freshly prepared $NaBH_4$ (final concentration 24 μM) was rapidly added for reduction, and silver clusters were obtained after 24 h in the dark at room temperature.

2.3. Measurements

The absorption of DNA solution at 260 nm was recorded on an Eppendorf Biophotometer (Eppendorf AG 22331 Humburg, Germany). All fluorescence experiments were performed using a fluorescence spectrometer (F-4600, Hitachi Co. Ltd., Japan) with a Xenon lamp as excitation source, and slit widths for the excitation and emission were set at 10 and 10 nm respectively. Absorption spectra were recorded on a UV/Vis spectrometer (Lambda 25, PerkinElmer, USA) with Milli-Q water as the reference solution. The TEM images of AgNCs were acquired on a transmission electron microscope (FEI Tecnai G-20) at accelerating voltage 200 kV.

2.4. Quantum yield measurement

Fluorescence quantum yield of the AgNCs was calculated using Cresol purple as the standard (ST), Cresol purple absorbs and emits in the same spectral region and its QY was reported to be 53% in methanol. All solutions had an optical density below 0.05 at the excitation wavelength (585 nm) to minimize reabsorption and avoid absorbance saturation. The following equation was used for calculation, $QY_{NC} = QY_{ST}(I_{NC}/A_{NC})(A_{ST}/I_{ST})(\eta_{NC}/\eta_{ST})$, where I, A, and η are the integrated emission intensity, absorbance at excitation wavelength, and refractive index of the solvent.

3. Results and discussion

3.1. Detection feasibility

Finding a universal design for biosensing based on DNA-AgNCs, poses an interesting challenge, as the exact interaction between the AgNCs and the nucleic acid is not known in detail. Thus, the optimal folding state of the oligonucleotide for stabilization of a fluorescent species remains to be elucidated. Due to changes in the secondary structure of DNA, the fluorescent properties of DNA-AgNCs are significantly affected. It was expected to design a DNA-AgNCs-probe whose secondary structure will change by recognizing and bonding the target strand. And the altered DNA-AgNCs will have better signal expression ability. A DNA template of C65G (sequence were shown in Table S1 in the supporting information, SI) was used, which was expected to be a template of AgNCs at this study. The characteristic sequence of Norovirus RNA was used to be the detection target. A special probe was designed, because of its complementary ends, incorporated the C65G sequence and folded it to make a secondary structure changing. When the target strand was recognized, the double-stranded structure of probe was opened due to the bond of the target, causing the C65G sequence to be released. The experiment protocol was shown in Scheme 1A. The probe bonding with the target were compared to the original probe, when used to synthesize AgNCs, producing a higher fluorescence intensity, and the thus the probe was in “turn-on” mode.

HP8 (Table S1) was designed firstly, which has 8 base pairs complementary sequence at the two ends. Shown as Fig. 1A, target sequence templated AgNCs did not have fluorescence intensity. HP8 + Target had an increase in fluorescence intensity compared to HP8, but the enhancement effect was not significant due to the large background signal. A question was proposed, whether increasing the length of the complementary sequence will reduce the background signal, the HP12-1 was designed because of that. As shown in Fig. 1B, it was found that the enhancement effect increased. But it suggested that only increasing the length of the complementary sequence did not reduce the background signal. At the same time, the HP12-2 was devised, which added 4 G (Guanine) to the sequence to form a complementary sequence with 4C (Cytosine) bases in the C65G sequence. As shown in

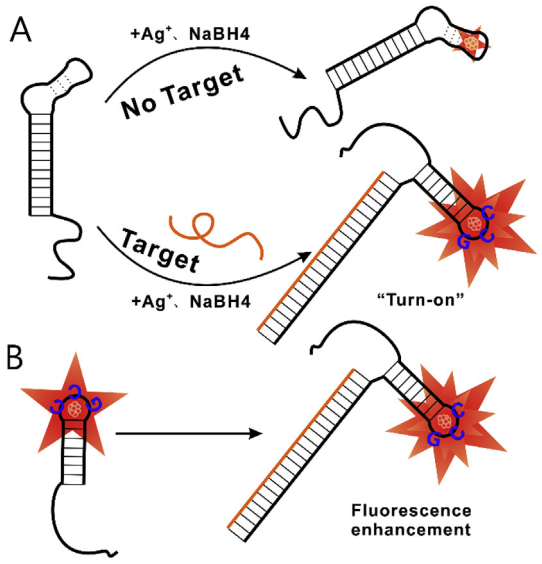

Scheme 1. A. Schematic illustration of the label-free assay for RNA detection. Working principle: Target DNA hybridizes with probe leading to the change of DNA secondary structure. Releasing the synthesis template of AgNCs. The GCC-loop could be used to synthesize AgNCs with high fluorescence intensity by adding Ag^+, $NaBH_4$. B. Additional double-stranded portion enhanced fluorescence intensity of GCC-loop templated AgNCs.

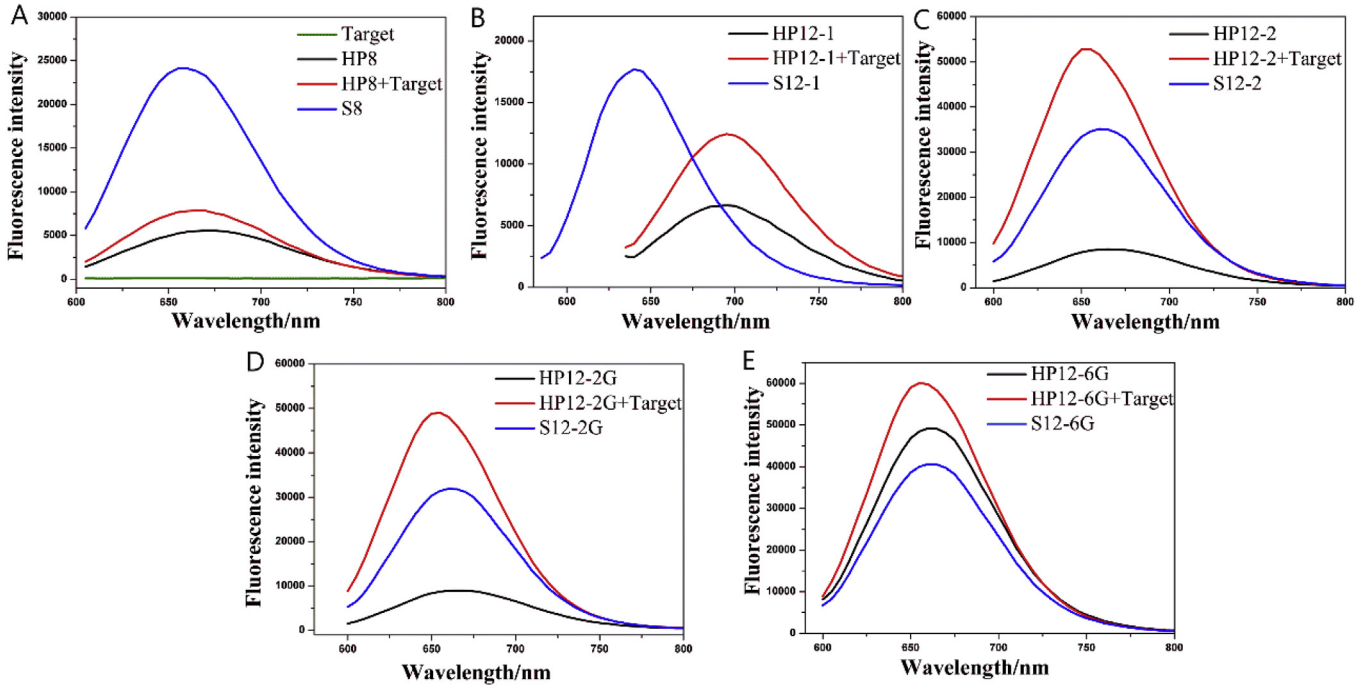

Fig. 1. Fluorescence spectra of AgNCs synthesized by five sets of DNA sequences respectively. Green line: fluorescence spectrum of Target templated AgNCs, black line: fluorescence spectrum of probe, red line: fluorescence spectrum of probe + target, blue line: fluorescence spectrum of S (the part of the probe + target removed the double chain). A. HP8 group; B. HP12-1 group; C. HP12-2 group; A. HP12-2G group; A. HP12-6G group. (For interpretation of the references to colour in this figure legend, the reader is referred to the Web version of this article.)

Fig. 1C, there was a gratifying change, although the background signal did not decrease, the fluorescence signal of the probe + target increased significantly. The fluorescence intensity of HP-12-2 + target was larger than S12-2. S8, S12-1, and S12-2 are the portions of HP8 + Target, HP12-1 + Target, and HP12-2 + Target after removing the double-strand, respectively (shown in Fig. 2). Since fully complementary dsDNA did not provide sufficient space for the bond of AgNCs, there was little fluorescence after the addition of Ag^+ [20]. Therefore, it was believed that the fluorescence signal of AgNCs were generated in the parts of S8, S12-1, and S12-2. When the target was added, not only the fluorescence intensity changed, but also the fluorescence peak positions of the respective groups were greatly different.

To illustrate the reasons for these phenomena, the DNA secondary structure of each group was analyzed on NUPACK website, the results were shown in Fig. 2A–C. It was found that C2 and C3 have very stable secondary structures compared to the other sequences, this was related to their good fluorescence properties. It was speculated that the hairpin structure named GCC-loop in the red dashed box is the main part utilized to generate the fluorescent AgNCs. There were many reports on the excellent properties of hairpin structures for the synthesis of AgNCs, and almost all of them were C6-loop [21,28]. Additionally, the GCC-loop we found is a good template for AgNCs synthesis. The DNA secondary structure of C2 altered a lot compared with C1, which was the main factor leading to a violent change in the fluorescence signal of the final synthetic AgNCs. Fig. 1C illustrated that the fluorescence intensity of C2 was significantly greater than that of C3, which can only be attributed to the enhanced function of the double-stranded portion, shown as Scheme 1B. Lin [29] once proposed a method for constructing stable DNA-AgNCs by attaching double-stranded portions, the fluorescence was enhanced by linking the double-stranded DNA structure to the template sequence of the AgNCs.

Due to the successful design of the HP12-2 sequence, the number of G complementary to C bases in C65G was studied, being 2G, 4G, 6G, respectively. 2G is HP-12-2G, 4G corresponded to HP12-2, and 6G amounts to HP-12-2G. As shown in Fig. 1, the results of HP12-2G are similar to those of HP12-2 when the fluorescence intensity of HP12-6G significantly increased. Meanwhile, the NUPACK was applied to analyze the secondary structure of those DNA sequences, shown as Fig. 2C–E. With the exception of C1 and D1, all sequences had stable GCC-loop, corresponding to their strong fluorescence. Owing to the change of the secondary structure of E1 relative to D1 and C1 in Fig. 2, the fluorescence intensity of HP12-6G in Fig. 1 remarkably increased in comparison to HP12-2G and HP12-2. Enhancing the fluorescence intensity of the AgNCs by attaching double-strand portion resulted in the increase of the fluorescence intensity of HP12-6G + Target relative to HP12-6G. The fluorescence intensity of C2, D2, and E2 are 0.5654 times higher than that of C3, D3, and E3, due to the enhancement function of double-strand, shown as Table S3. According to the above analysis of the experiment principle, it is reasonably believed that the fluorescence enhancement of HP12-2 + Target relative to HP12-2 was attributed to three aspects: 1. The existence of GCC-loop; 2. Stable secondary structure; 3. The enhancement function of additional double-strand.

Comparing D3, C3, E3, E1, it was found that the length of the stem of the GCC-loop gradually increased, in the same way, the fluorescence intensity varied accordingly. Probably because longer stems provide a better microenvironment for AgNCs [30], reducing the occurrence of quenching in solution [31]. It is a good discovery which can provide some reference value for the synthesis of DNA-AgNCs. The experiment data of the five probes were summarized in Table S2, HP12-2 was selected as a probe for subsequent experiments.

3.2. Optimization of detection conditions

The experiment conditions were optimized for higher detection sensitivity. Firstly, the pH of the Phosphate buffer solution was tested. The results were shown in Fig. 3A, while the fluorescence spectrum was shown in Fig. S1. The error bars represented the standard deviation, and the black part represented the fluorescence intensity of HP12-2. When the pH was less than 7, the fluorescence intensity of HP12-2 increased with the increase of pH, and when the pH was greater than 7,

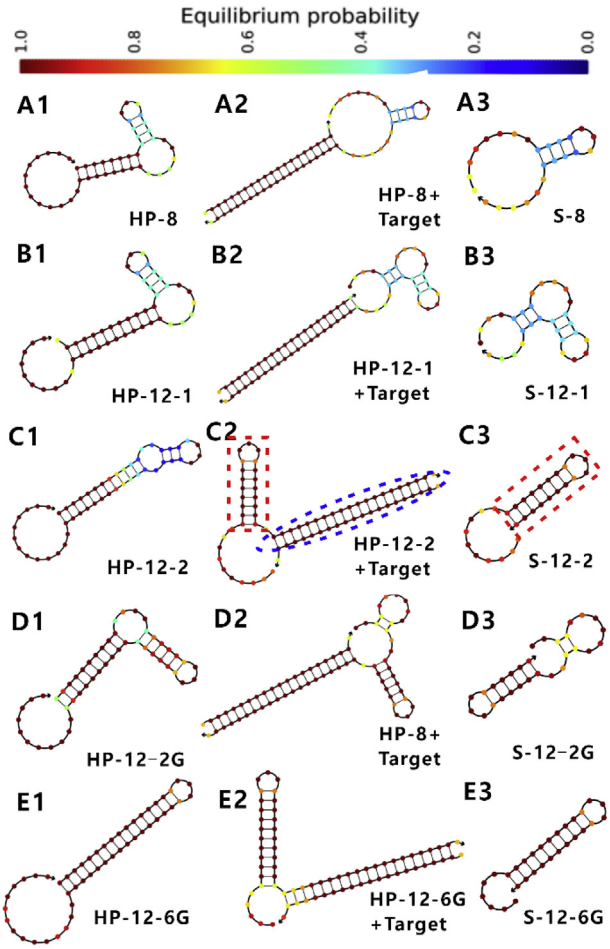

Fig. 2. Secondary structure diagram predicted by each sequence on NUPACK website. As shown in the legend, the colour represents the strength of the bond. Red dotted frame represents GCC-loop; Blue dotted frame represents an additional double-stranded structure. (For interpretation of the references to colour in this figure legend, the reader is referred to the Web version of this article.)

it decreased with the increase of pH. Red + black on behalf of the fluorescence intensity of HP-12-2 + Target, it was found that its fluorescence intensity at pH 6.6 was significantly greatest, indicating that the suitable synthesis buffer environment for GCC-loop was pH6.6. The possible reason is that C (cytosine) has the best binding ability to AgNCs [32], and C has better binding ability to Ag^+ under weakly acidic conditions when N3 sites are deprotonated [33]. The red portion represented the increased fluorescence intensity of HP12-2 + Target relative to HP-12-2, it was observed that the maximum enhancement was at pH 6.6. The conditions of pH6.6 were selected for subsequent experiments.

Next, the ratio of concentration of DNA:$AgNO_3$ was researched, and the fluorescence intensity was measured at 480/585 nm. As shown in Fig. 3B, the fluorescence intensity of HP12-2 + Target first increased and then decreased as the concentration of Ag^+ increased. Achieved a maximum at the condition of DNA:$AgNO_3$ = 1:12. The fluorescence spectrum was shown in Fig. S2. At the beginning, the fluorescence intensity increased with the increase of Ag^+. May be because of that the Ag^+ in the loop did not reach the satisfying concentration for forming the fluorescence AgNCs. That is, with the increasing concentration of Ag^+, the fluorescence intensity strengthened as the number of AgNCs of synthetic luminescence increased. When the concentration of Ag^+ reached saturation, as the concentration increased, the fluorescence AgNCs transformed into a larger non-luminescent silver nanoparticles. At higher Ag^+ stoichiometry, the reduced fluorescence is attributed to

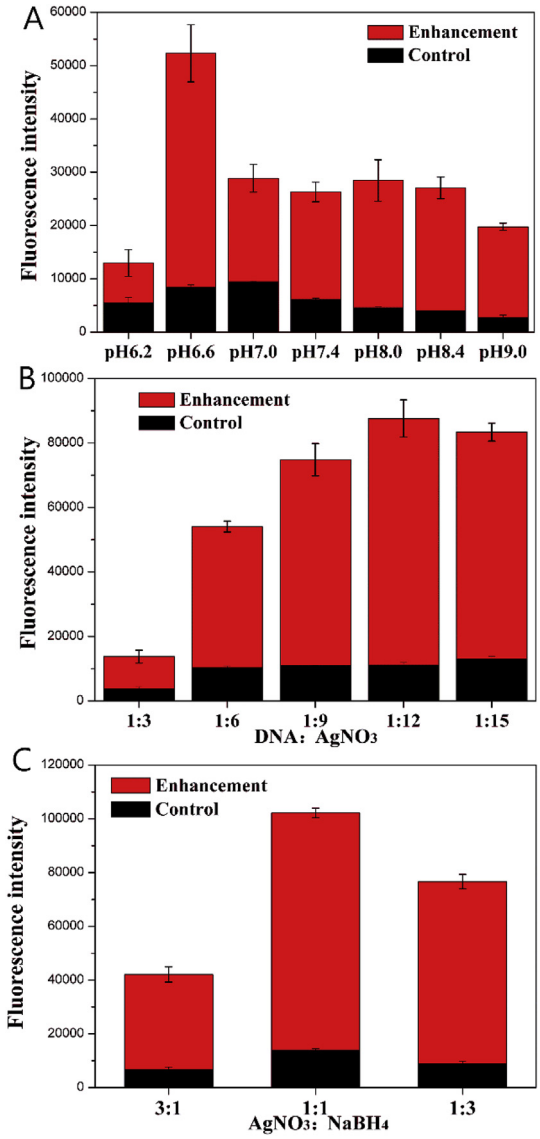

Fig. 3. Histogram of the results of optimized condition. A. different pH; B. different ratios of DNA and $AgNO_3$; C. different ratios of $AgNO_3$ and $NaBH_4$. Black: Fluorescence intensity of HP12-2; Red: enhanced fluorescence intensity of HP12-2 + Target relative to HP12-2. (For interpretation of the references to colour in this figure legend, the reader is referred to the Web version of this article.)

the formation of larger nanoparticles, depleting more and smaller fluorescent nanoclusters [32].

Reductants were essential in the synthesis of AgNCs, in a large number of literatures, $NaBH_4$ was used as a reducing agent in the synthesis of AgNCs with a condition of $AgNO_3$:$NaBH_4$ = 1:1 [34], 2:1 [35], 1:2 [23], or 3:1 [28]. Therefore, the effect of the ratio of $AgNO_3$:$NaBH_4$ in a certain range concerning the synthesis of AgNCs was studied. As shown in Fig. 3C, the fluorescence intensity of HP-12-2 + Target and HP-12-2 were both the largest at 1:1, but overall, the enhancement of fluorescence was also best at 1:1. While the ratio of $AgNO_3$ and $NaBH_4$ equals 1:3, the decrease in fluorescence intensity was attributed to the excessive reduction ability to convert some fluorescent AgNCs into larger non-fluorescent silver nanoparticles. When $AgNO_3$:$NaBH_4$ = 3:1, the reducing power was insufficient. The fluorescence spectrum was shown in Fig. S3.

Therefore, the optimized synthesis conditions were pH6.6, DNA: $AgNO_3$: $NaBH_4$ = 1:12:12. After optimization, the fluorescence intensity of HP12-2 + Target increased by 0.9344 times. The enhancement

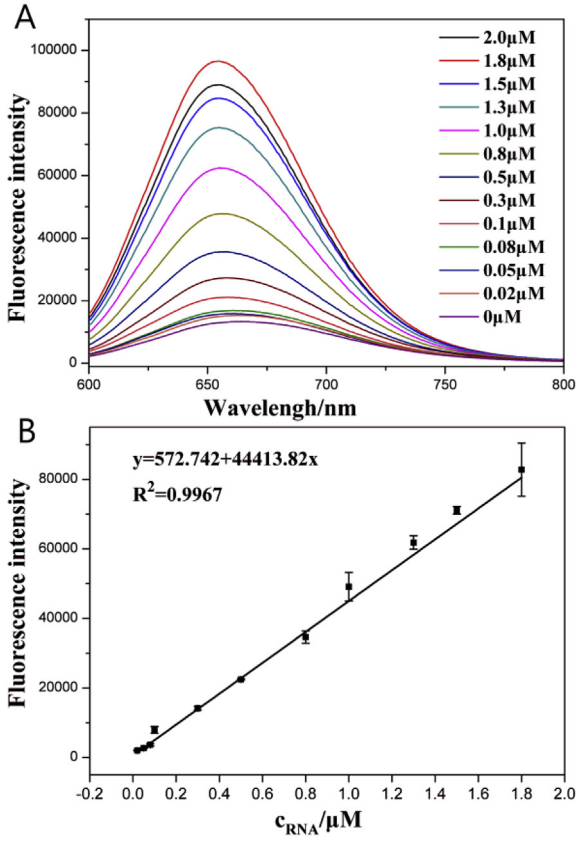

Fig. 4. A. Fluorescence emission spectra of AgNCs in the Presence of various concentrations of perfectly matched target RNA. B. Linear relation between the fluorescence signal ($FI_{HP12\text{-}2+Target}$-$FI_{HP12\text{-}2}$, FI: fluorescence intensity) and target concentration. Fluorescence intensities were recorded at 655 nm with an excitation Wavelength of 585 nm.

factor of HP12-2 + Target relative to HP12-2 increased from 4.8130 to 6.3108. The optimized results demonstrated that the optimizaton had a good effect on the detection of the target strand.

In order to characterize the HP12-2 + Target template AgNCs, a representative TEM image was taken and shown in Fig. S5, and the size of AgNCs is basically around 2 nm. At the same time, the quantum yield of the HP12-2 + Target template AgNCs was 51.60% by using Cresol purple as the standard, which was higher than most of the reported DNA-AgNCs.

3.3. Detection sensitivity and selectivity

Under the optimized conditions, we conducted experiments on detection range. As shown in Fig. 4A, between 0 and 2 μM, the fluorescence intensity of the system strongly depends on the concentration of the target strand, which further demonstrated that the experiment principle owing to the change in secondary structure caused by the binding of HP12-2 to the target strand, resulting in the changing of the fluorescence intensity of the AgNCs. As long as the concentration of the target chain increased, the fluorescence intensity of the system shall have corresponding increase, reaching the maximum at around 1.8 μM. The concentration of HP12-2 was 2.0 μM, and HP12-2 was a 1:1 combination with Target, therefore, the maximum limit of theoretical detection was 2 μM, which was consistent with the actual experiment data. Fig. 4B revealed the fluorescence signal changes of probe mixture as a function of the concentration of target RNA, the excellent linear relationship (R^2 = 0.9967) was established in the range from 20 nM to 1.8 μM by the linear equation, y = 572.742 + 44413.82x. The detection limit was 18 nM (taken to be three times the standard deviation).

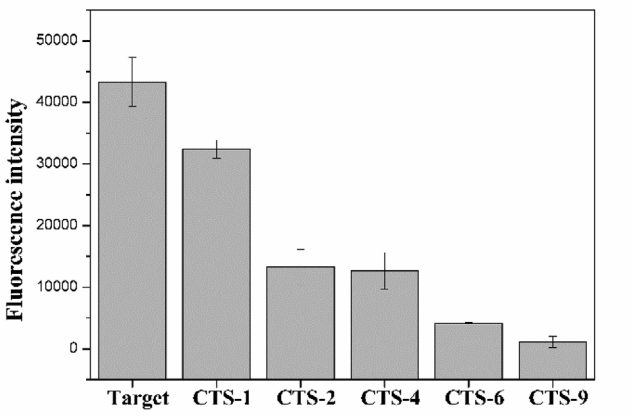

Fig. 5. Specificity of the RNA assay detecting different target. Control: no Target DNA was added; Target: perfectly matched target DNA; CTS-1: one-base mismatched DNA; CTS-2: two-base mismatched DNA; CTS-4: four-base mismatched DNA; CTS-6: six-base mismatched DNA; CTS-9: nine-base mismatched DNA. The DNA concentrations of Target, CTS-1, CTS-2, CTS-4, CTS-6, CTS-9 were 1 μM. Y-axis: Fluorescence signal changes ($FI_{HP12\text{-}2+Target}$-$FI_{HP12\text{-}2}$).

We then investigated the selectivity of this DNA hairpin probe system. Fig. S4 showed the fluorescence spectrum of the system after adding different target strands, and Fig. 5 illustrated the increase in system fluorescence intensity relative to the control group. As shown, great fluorescence increase was obtained thanks to the addition of perfectly matched RNA. However, the increase intensity for one-base mismatched RNA was only about 74.80% of that for perfect target at the same condition, and the increase intensity for two-base mismatched RNA was only about 30.74%. As the number of mismatched bases increased, the enhancement effect of the fluorescence intensity sharply decreased. When there were more than four base mismatches, the fluorescence intensity of the system after adding the target strand was almost the same as that of the control group, and no significant fluorescence enhancement can be observed. The reason was that as the number of the mismatched bases increased, the binding ability of RNA diminished, hence, the amount of RNA bound to the system decreased. When the number of mismatched bases increased to more than 4 bases, the mismatched RNA was insufficient to open the double-stranded structure of the probe, so that the secondary structure of the probe cannot be changed to yield the fluorescence enhancement effect. These results indicate that this RNA detection platform can provide an excellent capability in differentiating between perfectly matched and mismatched RNA targets, demonstrating the good selectivity of this platform.

Finally, the recovery test was conducted and the results were listed in Table 1. We chose three appropriate concentrations of linear range to conduct recovery test: 0.50, 1.0, and 1.5 μM. The recovery was 94.12–105.23% and the relative standard deviation was 2.89–4.82%. The results indicated that this detection method has good accuracy and can be applied to actual sample testing.

Table 1
Recovery analysis of Norovirus RNA.

Sample	Added (μM)	Found (μM)	Recovery (%)	RSD (%)
1	0.5	0.4706	94.12	4.82
2	1.0	1.0523	105.23	3.45
3	1.5	1.5186	101.24	2.89

4. Conclusions

In summary, it was found that the probe with a GCC-loop can be used to synthesize AgNCs with excellent optical properties of a 51.60% quantum yield through sequence design and principle analysis. The fluorescence effect of GCC-loop-AgNCs was enhanced by the additional double-strand. A label-free Norovirus RNA detection platform was demonstrated as follows: DNA-AgNCs-probe can bind to the target chain to change its secondary structure, thus leading to an increase in fluorescence intensity. The detection limit of Norovirus RNA can be as low as 18 nM, and there was a linear relationship between 20 nM and 1.8 μM. Moreover, this detection platform was also selective to differentiate mismatched RNA, which makes it promising for detection applications. This detection system based on DNA-AgNCs-probe avoid chemical modification and is easy to operate, critically, no sophisticated experimental techniques is required. The assay can be accomplished by using a common spectrophotometer. At the same time, it only needs to change the recognition sequence of probe, which will be a universal method for different RNA detection.

Acknowledgement

This work was supported by the National Science Foundation of China (No. 31601552), the National Key Research and Development Program of China (No. 2017YFC1601704, 2018YFC1602300), the Key Research & Development Plan of Jiangsu Province (No.BE2016664), National first-class discipline program of Food Science and Technology (JUFSTR20180509), and the “HongKong Scholar” program.

Appendix A. Supplementary data

Supplementary data to this article can be found online at https://doi.org/10.1016/j.ab.2019.113365.

References

[1] J.R. Johnson, Foodborne illness acquired in the United States, Emerg. Infect. Dis. 17 (2011) 7–15.
[2] M.M. Patel, A.J. Hall, J. Vinje, U.D. Parashar, Noroviruses: a comprehensive review, J. Clin. Virol. 44 (2009) 1–8.
[3] A. Giamberardino, M. Labib, E.M. Hassan, J.A. Tetro, S. Springthorpe, S.A. Sattar, M.V. Berezovski, M.C. DeRosa, Ultrasensitive norovirus detection using DNA aptasensor technology, PLoS One 8 (2013) e79087.
[4] R.L. Atmar, T.G. Metcalf, F.H. Neill, M.K. Estes, Detection of enteric viruses in oysters by using the polymerase chain reaction, Appl. Environ. Microbiol. 59 (1993) 631.
[5] A. Fraisse, F. Niveau, C. Hennechart-Collette, C. Coudray-Meunier, S. Martin-Latil, S. Perelle, Discrimination of infectious and heat-treated norovirus by combining platinum compounds and real-time RT-PCR, Int. J. Food Microbiol. 269 (2018) 64–74.
[6] K. Kumthip, P. Khamrin, W. Saikruang, K. Supadej, H. Ushijima, N. Maneekarn, Comparative evaluation of norovirus infection in children with acute gastroenteritis by rapid immunochromatographic test, RT-PCR and real-time RT-PCR, J. Trop. Pediatr. 63 (2017) 468–475.
[7] H.G. Cho, S.G. Lee, S.K. Mun, M.J. Lee, P.H. Park, W.H. Jheong, M.H. Yoon, S.Y. Paik, Detection of waterborne norovirus genogroup I strains using an improved real time RT-PCR assay, Arch. Virol. 162 (2017) 3389–3396.
[8] X. Gao, Z. Wang, Y. Wang, Z. Liu, X. Guan, Y. Ma, H. Zhou, Y. Jiang, W. Cui, L. Wang, Y. Xu, Surveillance of norovirus contamination in commercial fresh/frozen berries from Heilongjiang Province, China, using a TaqMan real-time RT-PCR assay, Food Microbiol. 82 (2019) 119–126.
[9] S.R. Ahmed, K. Takemeura, T.C. Li, N. Kitamoto, T. Tanaka, T. Suzuki, E.Y. Park, Size-controlled preparation of peroxidase-like graphene-gold nanoparticle hybrids for the visible detection of norovirus-like particles, Biosens. Bioelectron. 87 (2017) 558–565.
[10] J.H. Kim, J.E. Park, M. Lin, S. Kim, G.H. Kim, S. Park, G. Ko, J.M. Nam, Sensitive, quantitative naked-eye biodetection with polyhedral Cu nanoshells, Adv. Mater. 29 (2017).
[11] P. Weerathunge, R. Ramanathan, V.A. Torok, K. Hodgson, Y. Xu, R. Goodacre, B.K. Behera, V. Bansal, Ultrasensitive colorimetric detection of murine norovirus using NanoZyme aptasensor, Anal. Chem. 91 (2019) 3270–3276.
[12] M.N. Karim, S.R. Anderson, S. Singh, R. Ramanathan, V. Bansal, Nanostructured silver fabric as a free-standing NanoZyme for colorimetric detection of glucose in urine, Biosens. Bioelectron. 110 (2018) 8–15.
[13] F. Chen, F. Tang, C.T. Yang, X. Zhao, J. Wang, B. Thierry, V. Bansal, J. Dai, X. Zhou, Fast and highly sensitive detection of pathogens wreathed with magnetic nanoparticles using dark-field microscopy, ACS Sens. 3 (2018) 2175–2181.
[14] L. Shang, S. Dong, G.U. Nienhaus, Ultra-small fluorescent metal nanoclusters: synthesis and biological applications, Nano Today 6 (2011) 401–418.
[15] L. Zhang, E. Wang, Metal nanoclusters: new fluorescent probes for sensors and bioimaging, Nano Today 9 (2014) 132–157.
[16] J.P. Wilcoxon, B.L. Abrams, Synthesis, structure and properties of metal nanoclusters, Chem. Soc. Rev. 35 (2006) 1162–1194.
[17] Y. Guo, F. Shen, Y. Cheng, Y. Xie, H. Yu, W. Yao, H.W. Li, H. Qian, R. Pei, The light-up fluorescence of AgNCs in a "DNA bulb, Nanoscale 10 (2018) 11517–11523.
[18] C.I. Richards, S. Choi, J.C. Hsiang, Y. Antoku, T. Vosch, A. Bongiorno, Y.L. Tzeng, R.M. Dickson, Oligonucleotide-stabilized Ag nanocluster fluorophores, J. Am. Chem. Soc. 130 (2008) 5038–5039.
[19] C.M. Ritchie, K.R. Johnsen, J.R. Kiser, Y. Antoku, R.M. Dickson, J.T. Petty, Ag nanocluster formation using a cytosine oligonucleotide template, J. Phys. Chem. C 111 (2007) 175–181.
[20] Z. Huang, F. Pu, D. Hu, C. Wang, J. Ren, X. Qu, Site-specific DNA-programmed growth of fluorescent and functional silver nanoclusters, Chemistry 17 (2011) 3774–3780.
[21] E.G. Gwinn, P. O'Neill, A.J. Guerrero, D. Bouwmeester, D.K. Fygenson, Sequence-dependent fluorescence of DNA-hosted silver nanoclusters, Adv. Mater. 20 (2008) 279–283.
[22] L. Feng, Z. Huang, J. Ren, X. Qu, Toward site-specific, homogeneous and highly stable fluorescent silver nanoclusters fabrication on triplex DNA scaffolds, Nucleic Acids Res. 40 (2012) e122.
[23] B. Sengupta, K. Springer, J.G. Buckman, S.P. Story, O.H. Abe, Z.W. Hasan, Z.D. Prudowsky, S.E. Rudisill, N.N. Degtyareva, J.T. Petty, DNA templates for fluorescent silver clusters and I-motif folding, J. Phys. Chem. C 113 (2009) 19518–19524.
[24] J. Ai, W. Guo, B. Li, L. Tao, L. Dan, E. Wang, DNA G-quadruplex-templated formation of the fluorescent silver nanocluster and its application to bioimaging, Talanta 88 (2012) 450–455.
[25] J. Sharma, H.C. Yeh, H. Yoo, J.H. Werner, J.S. Martinez, Silver nanocluster aptamers: in situ generation of intrinsically fluorescent recognition ligands for protein detection, Chem. Commun. 47 (2011) 2294–2296.
[26] X. Liu, F. Wang, R. Aizen, O. Yehezkeli, I. Willner, Graphene oxide/nucleic-acid-stabilized silver nanoclusters: functional hybrid materials for optical aptamer sensing and multiplexed analysis of pathogenic DNAs, J. Am. Chem. Soc. 135 (2013) 11832–11839.
[27] G. Liu, J. Li, D.Q. Feng, J.J. Zhu, W. Wang, Silver nanoclusters beacon as stimuli-responsive versatile platform for multiplex DNAs detection and aptamer-substrate complexes sensing, Anal. Chem. 89 (2017) 1002–1008.
[28] P.R. O'Neill, L.R. Velazquez, D.G. Dunn, E.G. Gwinn, D.K. Fygenson, Hairpins with poly-C loops stabilize four types of fluorescent Ag n:DNA, J. Phys. Chem. C 113 (2009) 4229–4233.
[29] R. Lin, G. Tao, Y. Chen, M. Chen, F. Liu, N. Li, Constructing a robust fluorescent DNA-stabilized silver nanocluster probe module by attaching a duplex moiety, Chemistry 23 (2017) 10893–10900.
[30] L. Yang, C. Yao, F. Li, Y. Dong, Z. Zhang, D. Yang, Synthesis of branched DNA scaffolded super-nanoclusters with enhanced antibacterial performance, Small 14 (2018) e1800185.
[31] S.V. Rempel, A.A. Podkorytova, A.A. Rempel, Concentration quenching of fluorescence of colloid quantum dots of cadmium sulfide, Phys. Solid State 56 (2014) 568–571.
[32] V. Soto-Verdugo, H. Metiu, E. Gwinn, The properties of small Ag clusters bound to DNA bases, J. Chem. Phys. 132 (2010) 195102.
[33] B. Sengupta, C. Ritchie, J. Buckman, K. Johnsen, P. Goodwin, J. Petty, Base-directed formation of fluorescent silver clusters, J. Phys. Chem. C 112 (2008) 18776–18782.
[34] P. Shah, A. Rorvig-Lund, S.B. Chaabane, P.W. Thulstrup, H.G. Kjaergaard, E. Fron, J. Hofkens, S.W. Yang, T. Vosch, Design aspects of bright red emissive silver nanoclusters/DNA probes for microRNA detection, ACS Nano 6 (2012) 8803–8814.
[35] T. Driehorst, P. O'Neill, P.M. Goodwin, S. Pennathur, D.K. Fygenson, Distinct conformations of DNA-stabilized fluorescent silver nanoclusters revealed by electrophoretic mobility and diffusivity measurements, Langmuir 27 (2011) 8923–8933.